Nanoscale Res Lett (2007) 2:6–11
DOI 10.1007/s11671-006-9021-9

NANO EXPRESS

A solid-phase dot assay using silica/gold nanoshells

Boris Khlebtsov · Lev Dykman · Vladimir Bogatyrev · Vladimir Zharov · Nikolai Khlebtsov

Published online: 17 November 2006

Abstract We report on the first application of silica-gold nanoshells to a solid-phase dot immunoassay. The assay principle is based on staining of a drop (1 μl) analyte on a nitrocellulose membrane strip by using silica/gold nanoshells conjugated with biospecific probing molecules. Experimental example is human IgG (hIgG, target molecules) and protein A (probing molecules). For usual 15-nm colloidal gold conjugates, the minimal detectable amount of hIgG is about 4 ng. By contrast, for nanoshell conjugates (silica core diameter of 70 nm and gold outer diameter of 100 nm) we have found significant increase in detection sensitivity and the minimal detectable amount of hIgG is about 0.5 ng. This finding is explained by the difference in the monolayer particle extinction.

B. Khlebtsov · V. Bogatyrev · N. Khlebtsov (✉)
Lab of Nanoscale Biosensors, Institute of Biochemistry and Physiology of Plants and Microorganisms, Russian Academy of Sciences, 13 Pr. Entuziastov, Saratov 410049, Russia
e-mail: khlebtsov@ibppm.sgu.ru

V. Bogatyrev · N. Khlebtsov
Saratov State University, 155 Moskovskaya St, Saratov 410026, Russia

L. Dykman
Immunotechnology Group, Institute of Biochemistry and Physiology of Plants and Microorganisms, Russian Academy of Sciences, 13 Pr., Entuziastov, Saratov 410049, Russia

V. Zharov
Philips Classic Laser Laboratories, University of Arkansas for Medical Sciences, 4301 W Markham, Little Rock, AR 72206, USA

Keywords Colloidal gold · Silica/gold nanoshells · Solid-phase immunoassay

Introduction

The solid-phase immunoassays are based on adsorption of antigens onto a solid substrate followed by binding of adsorbed target molecules with biospecific labels. For instance, ELISA [1] technique uses antibodies conjugated with enzymes to detect antigens adsorbed onto inner sides of microtitration plates. It is well known that the reliability of ELISA analyses can only be ensured by application of a special equipment and standard microplates and reagents [2]. In modified versions of solid-phase immunoassays, the microtitration plates are replaced with nitrocellulose membrane filters [3] or siliconized matrices [4] to adsorb various antigens. In the membrane version, the solid-phase immunoassay can be called ''dot-immunoassay'' as usually a drop of analyte is deposited into center of a 5×5-mm delineate square and the reaction outcome looks like a colored dot. The simplicity of analyses and the saving of antigens and reagents allow one to implement the solid-phase immunoassays in the laboratory, field, or even domestic circumstances [5] to detect proteins (Western blotting) [6], DNA (Southern blotting) [7], or RNA (Northern blotting) [8].

In 1984, four independent publications [9] reported on using colloidal gold particles as labels for solid-phase immunoassay. The application of colloidal gold conjugates is based on visual detection of biospecific binding between adsorbed antigens and functionalized particles due to intense red color of markers [10]. In the ''golden'' dot-immunoassay, various biospecific

recognizing molecules can be used, including immunoglobulins [11, 12], Fab- and scFv antibody fragments [13], protein A [10], lectins [14], enzymes [15], streptavidin or antibiotin antibodies [16], etc. The colloidal gold conjugates have been applied to diagnostics of parasite [17], virus [18], and fungus [19] diseases, tuberculosis [20], melioidosis [21], syphilis [22], brucellosis [23], shigellosis, and other enteric bacterial infections [24], myocardial infarction [25], early pregnancy [26], species identification of bloodstains [27], dot-blot hybridization [28], and serotyping of soil bacteria [29].

In spite its attractive simplicity and efficiency, the colloidal gold dot-immunoassay is not free of drawbacks such as moderate sensitivity and long time of detection. Last years, various new types of nanoparticle structures have been suggested [30], including gold nanorods [31] and silica/gold nanoshells [32]. In particular, the silica/gold nanoshells have been used in analytical diagnostics [33], photothermal therapy [34], and optical visualization of cancer cells [35]. Here we report on the first, to the best of our knowledge, application of silica/gold nanoshells to a solid-phase dot assay in which the nanoshells are used as color markers for biospecific staining of a drop analyte placed on a nitrocellulose membrane strip. Other steps of dot assay technology being retained, the simple replacement of 15–30 nm gold nanospheres by silica/gold nanoshells results in dramatic (from four- to eight-fold) increase in the detection sensitivity.

Experimental section

For experiments presented in this paper, 15-nm colloidal gold nanospheres were prepared by Frens citrate reduction protocol [10], whereas gold nanoshells were fabricated as described in Ref. [36] with minimal modifications concerning concentration and amount of reagents. The extinction and elastic light scattering (at 90°) spectra of silica core and final nanoshell particles were measured as described previously [37] by using a Specord M 40 spectrophotometer equipped with a special attachment for differential light scattering spectroscopy measurements. To evaluate the silica core and nanoshell diameter distributions, we used the dynamic light scattering (DLS) setup described in Ref. [38]. The DLS setup includes a He–Ne laser (λ = 633 nm, 10 mW/mm^2), GO-5 goniometer (here the scattering angle was equal to 90°), the temperature control unit (±0.1°C), and a 288-chanel real-time correlator PhotoCor-SP (PhotoCor, Russia). The autocorrelation functions of scattered intensity fluctuations were measured with sample time 10^{-5} c for 1200 c. To solve the inverse DLS problem [39], we used the DynaLS algorithm [40]. In these experiments, we first evaluated the silica core size distributions. Then, after synthesis of gold nanoshells, the outer diameter distributions were measured. The gold shell thickness distribution can be obtained by subtraction of the shell and core size distributions.

Figure 1 shows an example of silica core and outer particle diameter distributions (Fig. 1a), as well as the measured and calculated light scattering spectra (Fig. 1b). Theoretical calculations were carried out by a multilayer Mie algorithm [41] with using the spectral dependence of water, silica, and gold dielectric functions as described in Ref. [42] (the bulk gold dielectric function was modified to account for the scattering of electrons at gold shell boundaries [42, 43]). Close agreement between the measured and calculated light scattering and extinction (not shown) spectra gives evidence for reliability of DLS nanoshell structure parameters.

As an example of biospecific molecular binding, we chose the human IgG (hIgG, Sigma, USA) and protein A (Sigma) pair. Protein A is a staphylococcal cell-wall protein that can interact, with a high affinity constant, with the Fc fragment of the IgG molecule. Each protein A molecule can bind at least two IgG molecules [44]. Two types of conjugates, CG-15 nm + ProteinA and NS-70/100 nm + Protein A were compared in our dot assay experiments. Designation CG-15 nm means 15-nm (in diameter) gold nanospheres, whereas symbol NS-70/100 nm stands for silica (70 nm in diameter)/gold (100 nm outer diameter) nanoshells.

Let us discuss first the general principles behind optical monitoring of nanoparticle functionalization. It is well known [45, 46] that each colloidal gold particle has a Au^0 core and a Au^I shell due to incomplete reduction at the nanoparticle surface. Citrate and chloride ions are coordinated to the Au^I shell. So, each gold particle is net anionically charged and thus the gold sol is stabilized by electrostatic repulsion forces. The addition of an electrolyte (e.g., 0.1% NaCl) to a 15-nm gold colloid will result in a decrease in the average interparticle distance because of charge screening effects. Therefore, when NaCl salt is added to a 15-nm gold colloid, the particles aggregate and the colloid color turns from red to blue. The physical origin of pronounced changes in sol color and in extinction spectra is the strong electrodynamic interaction of gold particles, caused by their close proximity [47]. This not only serves as a simple demonstration of the charged nature of the particles but also shows how one can

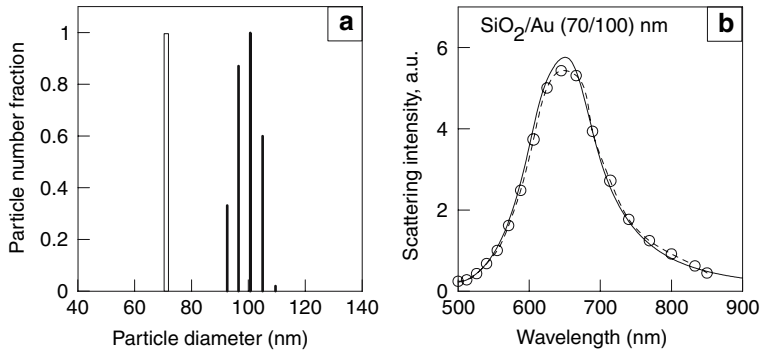

Fig. 1 (**a**) Particle diameter distributions measured by DLS method for silica core (white column) and silica/gold nanoshells (black columns). (**b**) Calculated (solid line) and measured (dashed line, circles) light scattering spectra of 70/100 nm silica/gold nanoshells

optically monitor the particle surface functionalization. Indeed, the addition of protein A to the 15-nm gold sol and the attachment of protein A molecules to the particle surface results in steric stabilization [48] of particles that now do not aggregate after addition of the same electrolyte quantity. Therefore, the polymer stabilization of gold nanoparticles against the salt aggregation can be considered as a direct indication of biopolymer modification of the colloidal gold particle surface. In the case of silica/gold nanoshells, the optical monitoring is not as evident as in the case of small solid gold particles. The reason is that the colors of nonaggregated (stabilized) and aggregated sols are similar. Nevertheless, the extinction spectra of the initial, functionalized, and aggregated nanoshells can be used for quantitative optical control of nanoparticle functionalization. In this work, the surface protein A functionalization of silica/gold nanoshells was verified by the minor spectral salt-induced changes of stabilized particles, by the positive interaction with complementary analyte (hIgG) molecules in solid-phase dot-immunoassay, and by the absence of interaction with a negative control (BSA).

The protocol for obtaining CG-15 nm + Protein A conjugates, which includes preparation and purification of an aqueous probe solution, determination of the ''gold number'' (minimum amount of protein that protects the sol against salt aggregation), attachment of the probe to the label, addition of a secondary stabilizer, concentration of the marker, and optimization of the end product, was described in detail elsewhere [10]. The resonance optical density A_{515} of 15-nm gold sol at 515 nm was adjusted to 1 (the sol thickness equals 1 cm). This solution has the following parameters: the particle extinction and scattering cross sections are $C_{\text{ext}}(\lambda = 515\,\text{nm}) \simeq 1.6 \times 10^2\,\text{nm}^2$ and $C_{\text{sca}}(\lambda = 515\,\text{nm}) \simeq 0.5\,\text{nm}^2$, respectively, the particle number concentration $N \simeq 1.4 \times 10^{12}\,\text{cm}^{-3}$, and the total surface of all particles in $1\,\text{cm}^3$ $S = N\pi R^2 \simeq 2.5\,\text{cm}^2$. To obtain conjugates, 10 μg of protein A was added to a 1 ml of 15-nm gold sol. This amount of protein stabilizes sol against addition of NaCl (the final salt concentration is about 1%).

The resonance optical density A_{630} of nanoshell sol was equal to 1.4. Taking into account the DLS geometrical parameters of nanoshells, we obtain the extinction $C_{\text{ext}}(\lambda = 630\,\text{nm}) \simeq 6.8 \times 10^4\,\text{nm}^2$and scattering $C_{\text{sca}}(\lambda = 630\,\text{nm}) \simeq 4.2 \times 10^4\,\text{nm}^2$ cross sections, the particle number concentration $N \simeq 0.5 \times 10^{10}\ \text{cm}^{-3}$, and the total surface of all particles in $1\,\text{cm}^3$ $S = N\pi R^2 \simeq 0.4\,\text{cm}^2$. Virtually the same particle concentration was determined by relating the measured optical density of 70-nm silica nanospheres and their calculated extinction cross section $C_{\text{ext}}(\lambda = 500\,\text{nm}) \simeq 3.1\,\text{nm}^2$. As the total particle surface was significantly less than that in the case of 15-nm gold nanospheres, we assumed that the addition of 10 μg of protein A to a 1 ml of nanoshell sol should also stabilize it against salt aggregation. The absence of salt-induced aggregation can be controlled by absence of significant changes in extinction and scattering spectra after addition of salt. We do observed the stabilization of nanoshell conjugates against salt, and this finding can be considered as strong evidence for the attachment of protein A molecules to nanoshell surface. It can be assumed that the attachment of protein A to gold nanoshells is controlled by electrostatic interaction at the corresponding buffer conditions, according to the generally accepted mechanism for adsorption of other biopolymers to colloidal gold particles [10].

The dot assay was carried out on nitrocellulose membranes (0.45 μm pore size; Schleicher & Schuell, Germany). One microliter drops of the assay material (hIgG; Sigma, USA) were spotted onto a nitrocellulose filter in the center of drawn 5 × 5-mm squares, and the membranes were held in a dry-air thermostat at 60°C for 15 min. Note that the size of a dot on the membrane strip is determined by the volume of analyte and by the membrane property, but not by the analyte concentration. In our experimental conditions (1 μl

analyte drops), the dot sizes were about 4–5 mm. After spotting, the filters were incubated for 30 min at room temperature in a blocking buffer (0.1% PEG, M_w = 20,000, Sigma, USA; 150 mN NaCl, and 20 mM TrisHCl, pH 8.2). This procedure prevents non-specific adsorption.

To detect hIgG, the nitrocellulose strip, after treatment as above, was placed in a parafilm envelope and was incubated in solutions of the CG-15 nm + Protein A or NS-70/100 nm + Protein A conjugates for 1 h at room temperature. The reaction outcome was the development of red or blue-gray spots at 5 min after adding the marker. The color of the spots intensified gradually over a period of 1 h. The strips were then removed and rinsed in water. Thereafter, they could be stored as long as was wished, without changes in staining intensity.

Figure 2 shows the results of dot assays with usual colloidal gold particles (Fig. 2a) and silica/gold nanoshells (Fig. 2b). The color of spots reflects the color of marker solutions. The first spot corresponds to 0.5 μg hIgG amount and other spots (first and second rows) were obtained by double dilutions so that the final spot corresponds to $0.5\,\mu g/2^{11} \simeq 0.2$ng of hIgG. The third row shows negative control with nonspecific BSA molecules taken at the same concentration as hIgG. Note that no staining occurred for spots with nonspecific BSA molecules. In the case of colloidal gold conjugates, the minimal detectable quantity of hIgG equals $C_{CG}^{min} = 0.5\,\mu g/2^7 \simeq 4$ng. By contrast, in the case of nanoshell conjugates, the minimal detectable quantity of hIgG lies between $C_{NS}^{min} = 0.5\,\mu g/2^{(9-10)} \simeq (0.5-1)$ng. Thus, a simple replacement of 15-nm gold nanospheres with 100-nm gold nanoshells results in dramatic increase in the dot assay sensitivity and the minimal detectable amount of hIgG molecules is about 0.5 ng.

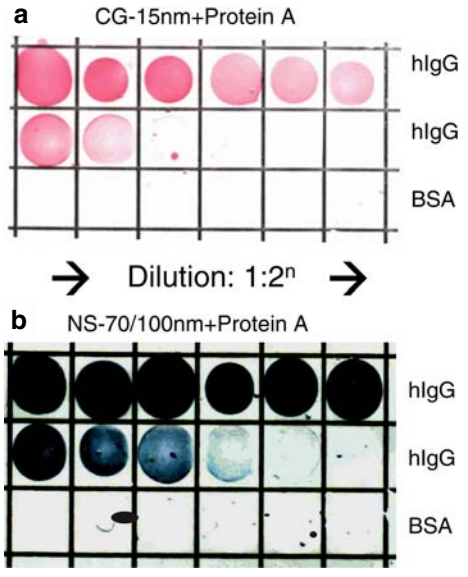

Fig. 2 Dot assay with colloidal gold (**a**) and nanoshell (**b**) conjugates. One microliter drops of hIgG (initial concentration 0.5μg/ml, sequential double dilutions $1:2^n$) were spotted onto a nitrocellulose filter in the center of drawn 5-mm squares. No staining occurs for the bovine serum albumin (BSA) that was used as negative control

Discussion

To give some insight into possible mechanisms behind observed difference in detection sensitivity, we first note that the minimal detectable analyte quantity does not depend on the concentration of probing markers although the concentration of markers affects the staining kinetics (data of our unpublished observations). This observation means that the main limiting factor for detection sensitivity is the amount of analyte sites available for biomolecular binding with recognizing molecules (protein A) attached to the particle surface. Let us suppose that the detection sensitivity at lowest analyte concentrations is determined by the single-particle extinction properties provided that there is some kind of proportionality between the available sites and number of specifically adsorbed markers. Then, by comparing the above extinction coefficients, one could expect the significant (about 4×10^2) increase in the detection sensitivity, which is at odds with our experimental data.

Another explanation may be an assumption that the detection limit corresponds to the single-layer assembling of markers and the ratio of detection sensitivity can be determined by equation

$$s \equiv s_{CG}^{NS} = \frac{N_{ads}^{rmNS} C_{ext}^{NS}}{N_{ads}^{CG} C_{ext}^{CG}} = \frac{Q_{ext}^{NS}}{Q_{ext}^{CG}} \quad (1)$$

where N_{ads}^{CG} and N_{ads}^{NS} are the numbers of single-layer adsorbed colloidal gold spheres and nanoshells, respectively; Q_{ext} is the extinction efficiency defined as the ratio of the extinction and geometrical cross sections. For resonance wavelengths, Eq. 1 predicts the estimate $s \simeq 8.6/0.9 \simeq 9.5$ in excellent agreement with our experimental observations.

Finally, we would like to discuss some points related to optimal properties of nanoparticles that may be used in the solid-phase dot immunoassay. In principle, the silica/gold nanoshells are not the only nanoparticle platform for analogous dot assays and the similar experiments may be still feasible with

other core materials, e.g. polystyrene/gold nanoshells [49]. However, in our opinion, the silica/gold nanoshells are the most convenient plasmon-resonant markers due to easy and reproducible preparation technology.

The next point concerns the core/shell geometrical parameters. Our choice (70/100 nm) can be considered as a compromise between the aggregation stability of nanoshells, their optimal optical properties, and functionalization ability. The nano-sized spherical SiO_2 cores can be easily fabricated using the Stöber method [50] with diameters ranging from 50–70 nm to 500 nm. On the other hand, the minimal gold shell thickness is usually about 15–20 nm [36]. Thus, the minimal outer diameter of nanoshells is about 100 nm. The extinction cross section of such nanoshells is more than two orders higher as compared to 15-nm colloidal gold spheres and in contrast to 100-nm solid gold spheres such particles do not sediment within 1–2 h. Furthermore, we have found that NS-70/100-nm nanoshells can be covered by protein A molecules without any chemical procedures, i.e. by using simple mixing of nanoshells and protein A solutions. One may assume that other core/shell structures with close (core diameter)/(shell thickness) ratios can be used as dot immunoassay markers. However, this point seems to be the subject of a separate special study.

With an increase in the gold shell thickness (or the shell/core ratio), the optical properties of nanoshells approach those for solid spheres. From this point of view, if the core/shell particles are replaced by pure gold particles with the same size, we also can expect an enhancement of the detection sensitivity in comparison with 15-nm colloidal gold particles. At present, there exist several technologies for controlled preparation of solid gold nanoparticles in a wide range of sizes (including 100–120-nm particles) [51]. However, the practical use of such large solid spheres may be inconvenient because of high sedimentation rate and unclear ability for functionalization through the simple adsorption route.

Finally, we note that the solid-phase dot-immunoassay can be considered a semi-quantitative technique, at least in its present form, as the assay allows one to determine of a minimal analyte quantity from a series of double dilutions. Nevertheless, we believe that the dot color intensity can be correlated with the analyte amount within a certain (possibly narrow) concentration range. To find a correlation between the analyte concentration and the color intensity, one needs to have an instrumental quantitative approach to measuring the color intensity. In our opinion, such a project could be realized in the future.

Conclusion

To summarize, we have shown that the silica gold nanoshells can be functionalized by the simple adsorption without any chemical derivation of attached molecules (thiol-, amine-, etc.). The functionalized nanoshells, being used as biospecific markers in dot immunoassay, reveal significantly high sensitivity compared to usual gold nanospheres. This experimental finding is in excellent agreement with a theoretical model based on comparison of the extinction cross sections of monolayer assembled markers. Although we have studied only one experimental biospecific pair (hIgG + protein A), the similar strategy could be possibly used for the detection of other target molecules. As it has been pointed out in the introduction section, the colloidal gold dot-immunoassay has been a well-known technique since 1984 [9]. However, to the best of our knowledge, this work can be considered the first report on the dot-immunoassay based on silica/gold nanoparticles rather than on colloidal gold markers.

Acknowledgments This research was partially supported by grants from RFBR (Nos.05-02-16776, 04-04-48224), the targeted program ''Research of cooperative and non-linear phenomena in light transport through mesascopic media as applied to development of diagnostical techniques in biology, medicine and industry'' (No. RNP.2.1.1.4473). BK was supported by grants from the President of Russian Federation (MK 961.2005.2), CRDF (BRHE Annex BF4M06 Y2-B-06-08), and INTAS Young Scientist Fellowship Grant 06-1000014-6421. VZ was supported by grants from the National Institute of Biomedical Imaging and Bioengineering (NIH/NIBIB, nos. EB000873 and EB0005123).

References

1. E. Engvall, P. Perlmann, J. Immunochem. **8**, 871 (1971)
2. B.S. Chessum, J.R. Denmark, Lancet **1**, 161 (1978); L.J. Kricka, T.J.N. Carter, S.M. Burt, J.H. Kennedy, R.L. Holder, M.I. Holliday, M.E. Telford, G.B. Wisdom, Clin. Chem. **26**, 741 (1980)
3. R. Hawkes, E. Niday, J. Gordon, Anal. Biochem. **119**, 142 (1982)
4. T. Furuya, K. Ikemoto, S. Kawauchi, A. Oga, S. Tsunoda, T. Hirano, K. Sasaki, J. Histochem. Cytochem. **52**, 205 (2004)
5. B.C. Walton, M.G. Pappas, M. Sierra, R. Hajkowski, P.R. Jacson, R. Custodio, Bull. P.A.H.O. **20**, 147 (1986)
6. W.N. Burnette, Anal. Biochem. **112**, 195 (1981)
7. E.M. Southern, J. Mol. Biol. **98**, 503 (1975)
8. J.C. Alwine, D.J. Kemp, G.R. Stark, Proc. Natl. Acad. Sci. U.S.A. **74**, 5350 (1977)
9. D. Brada, J. Roth, Anal. Biochem. **142**, 79 (1984); M. Moeremans, G. Daneles, A. van Dijck, G. Langanger, J. De Mey, J. Immunol. Meth. **74**, 353 (1984); B. Surek, E. Latzko, Biochem. Biophys. Res. Commun. **121**, 284 (1984); Y.-H. Hsu, Anal. Biochem. **142**, 221 (1984)

10. L.A. Dykman, V.A. Bogatyrev, Biochemistry (Moscow) **62**, 350 (1997)
11. S.R. Kimball, S.L. Rannels, M.B. Elenski, L.S. Jefferson, Immunol. Meth. **106**, 217 (1988)
12. M.V. Sumaroka, L.A. Dykman, V.A. Bogatyrev, N.V. Evseeva, I.S. Zaitseva, S.Yu. Shchyogolev, A.D. Volodarsky, J. Immunoassay **21**, 401 (2000)
13. J.F. Hainfeld, R.D. Powell, J. Histochem. Cytochem. **48**, 471 (2000); I.V. Volokhina, I.A. Sazonova, V.A. Velikov, M.I. Chumakov, Microbiol. Research **160**, 67 (2005)
14. W.P. Li, C. Zuber, J. Roth, Histochemistry **100**, 347 (1993)
15. E.A. Saman, Gene Anal. Technol. **3**, 1 (1986)
16. S. Tomlinson, A. Luga, E. Huguenel, N. Dattagupta, Anal. Biochem. **171**, 217 (1988)
17. Y.S. Liu, W.P. Du, Z.X. Wu, Int. J. Parasitol. **26**, 127 (1996)
18. V.S. Dar, S. Ghosh, S. Broor, J. Virol. Meth. **47**, 51 (1994)
19. A.C. Reboli, Clin. Microbiol. **31**, 518 (1993)
20. L. Vera-Cabrera, A. Rendon, M. Diaz-Rodriguez, V. Handzel, A. Laszlo, Clin. Diagn. Lab. Immunol. **6**, 686 (1999)
21. M. Kunakorn, B. Petchclai, K. Khupulsup, P. Naigowit, Clin. Microbiol. **29**, 2065 (1991)
22. Q. Huang, X. Lan, T. Tong, X. Wu, M. Chen, X. Feng, R. Liu, Y. Tang, Z. Zhu, J. Clin. Microbiol. **34**, 2011 (1996)
23. T.Yu. Zagoskina, E.Yu. Markov, A.I. Kalinovskii, E.P. Golubinskii, Zh Mikrobiol. Epidemiol. Immunobiol. (in Russian) **6**, 64 (1998)
24. L.A. Dykman, V.A. Bogatyrev, FEMS Immunol. Med. Microbiol. **27**, 135 (2000); V.A. Lazarchik, L.P. Titov, T.N. Vorob'eva, T.S. Ermakova, O.N. Vrublevskaya, N.V. Vlasik, Pros. Natl. Acad. Sci. of Belarus Republic, Ser. Medical Sciences (in Russian) **3**, 44 (2005)
25. H. Guo, J. Zhang, D. Yang, P. Xiao, N. He, Colloids and Surfaces B **40**, 195 (2005)
26. Z. Xu, Chung Hua I Hsueh Tsa Chih (Taipei) **72**, 216 (1992)
27. S. Matsuzawa, H. Kimura, Y. Itoh, H. Wang, T. Nakagawa, J. Forensic Sci. **38**, 448 (1993)
28. A.F. Cremers, N. Jansen in de Wal, J. Wiegant, R.W. Dirks, P. Weisbeek, M. van der Ploeg, J.E. Landegent, Histochemistry **86**, 609 (1987)
29. V.A. Bogatyrev, L.A. Dykman, L.Yu. Matora, S.I. Schwartsburd, FEMS Microbiol. Lett. **96**, 115 (1992)
30. M.-Ch. Daniel, D. Astruc, Chem. Rev. **104**, 293 (2004)
31. J. Pérez-Juste, I. Pastoriza-Santos, L.M. Liz-Marzán, P. Mulvaney, Coordination Chem. Rev. **249**, 1870 (2005); C.J. Murphy, T.K. Sau, A.M. Gole, C.J. Orendorff, J. Gao, L. Gou, S.E.; Hunyadi, T. Li, J. Phys. Chem. B **109**, 13857 (2005); C. Burda, X. Chen, R. Narayanan, M.A. El-Sayed, Chem. Rev. **105**, 1025 (2005)
32. L.R. Hirsch, A.M. Gobin, A.R. Lowery, F. Tam, R.A. Drezek, N.J. Halas, J.L. West, Ann. Biomed. Eng. **34**, 15 (2006)
33. L.R. Hirsch, J.B. Jackson, A. Lee, N. Halas, J. West, Anal. Chem. **75**, 2377 (2003)
34. L.R. Hirsch, R.J. Stafford, J.A. Bankson, S.R. Sershen, B. Rivera, R.E. Price, J.D. Hazle, N.J. Halas, J.L. West, Proc. Natl. Acad. Sci. U.S.A. **23**, 13549 (2003)
35. C. Loo, L. Hirsch, M. Lee, E. Chang, J. West, N. Halas, R. Drezek, Opt. Lett. **30**, 1012 (2005)
36. S.J. Oldenburg, R.D. Averitt, S.L. Westcott, N. Halas, Chem. Phys. Lett. **288**, 243 (1998)
37. N.G. Khlebtsov, V.A. Bogatyrev, L.A. Dykman, B.N. Khlebtsov, M. Ya.Krasnov, J. Quant, Spectrosc. Radiat. Transfer **89**, 133 (2004)
38. B.N. Khlebtsov, E.M. Chumakov, S.V. Semyonov, M.I. Chumakov, N.G. Khlebtsov, Proc. SPIE **5475**, 12 (2004)
39. B.J. Berne, R. Pecora, Dynamic Light Scattering with Application to Chemistry, Biology, and Physics. Dover Publ., Mineola (2002)
40. URL: http://www.protein-solutions.com
41. N.G. Khlebtsov, J. Quant, Spectrosc. Radiat. Transfer **89**, 143 (2004)
42. B.N. Khlebtsov, N.G. Khlebtsov, Proc. SPIE **6164**, 11 (2006)
43. C.G. Granqvist, O. Hunderi, Phys. Rev. B **30**, 47 (1978)
44. A.M. Egorov, M.M. Dikov, Mendeleev Chem. J. **27**, 381 (1982)
45. H.B. Weiser, *Inorganic Colloid Chemistry*. Wiley, New York (1933)
46. C.A. Mirkin, Inorg. Chem. **39**, 2258 (2000)
47. N.G. Khlebtsov, A.G. Melnikov, V.A. Bogatyrev, L.A. Dykman. Optical properties and biomedical applications of nanostructures based on gold and silver bioconjugates, In: Videen G, Yatskiv Ya S, Mishchenko M I (eds.), *Photopolarimetry in Remote Sensing*, NATO Science Series, II. Mathematics, Physics and Chemistry, vol. 161, Kluwer Academic Publishers, Dordrecht, pp. 265–308 (2004).
48. E.D. Goddard, B. Vincent (eds.), *Polymer Adsorption and Dispersion Stability*(Am Chem. Soc., Washington (DC), ACS Symp. Ser., 1984).
49. W. Shi, Y. Sahoo, M.T. Swihart, P.N. Prasad, Langmuir **21**, 1610 (2005)
50. W. Stöber, A. Fink, J. Colloid Interface Sci. **26**, 62 (1968)
51. J. Kimling, M. Maier, B. Okenve, V. Kotaidis, H. Ballot, A. Plech, J. Phys. Chem. B **110**, 15700 (2006)